SUPPLEMENTAL INFORMATION

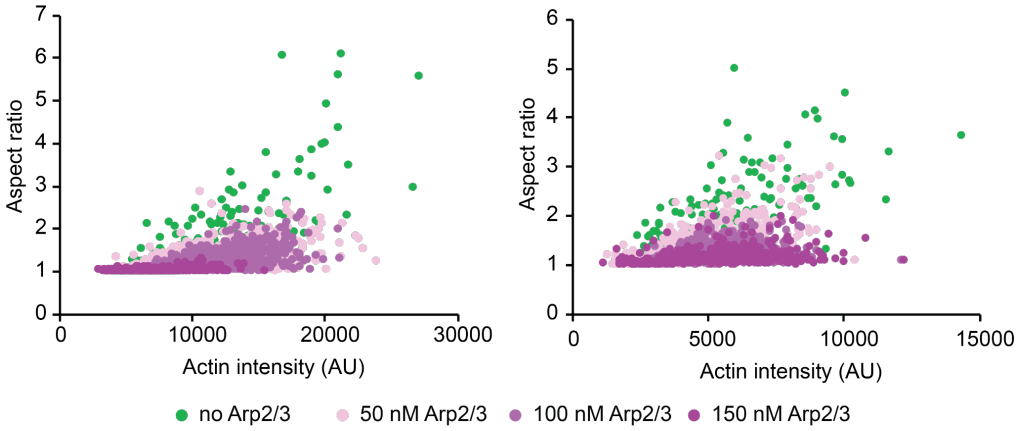

Supplemental Figure S1. Replicates of figure 3a. Relationship between droplet aspect ratio and actin intensity within the droplet for droplets formed from 15 μM VASP and exposed to 2 μM actin with increasing concentrations of Arp2/3 and VCA, as visualized in Figure 2a. *Left:* n = 3387 droplets. *Right:* n= 2761 droplets.

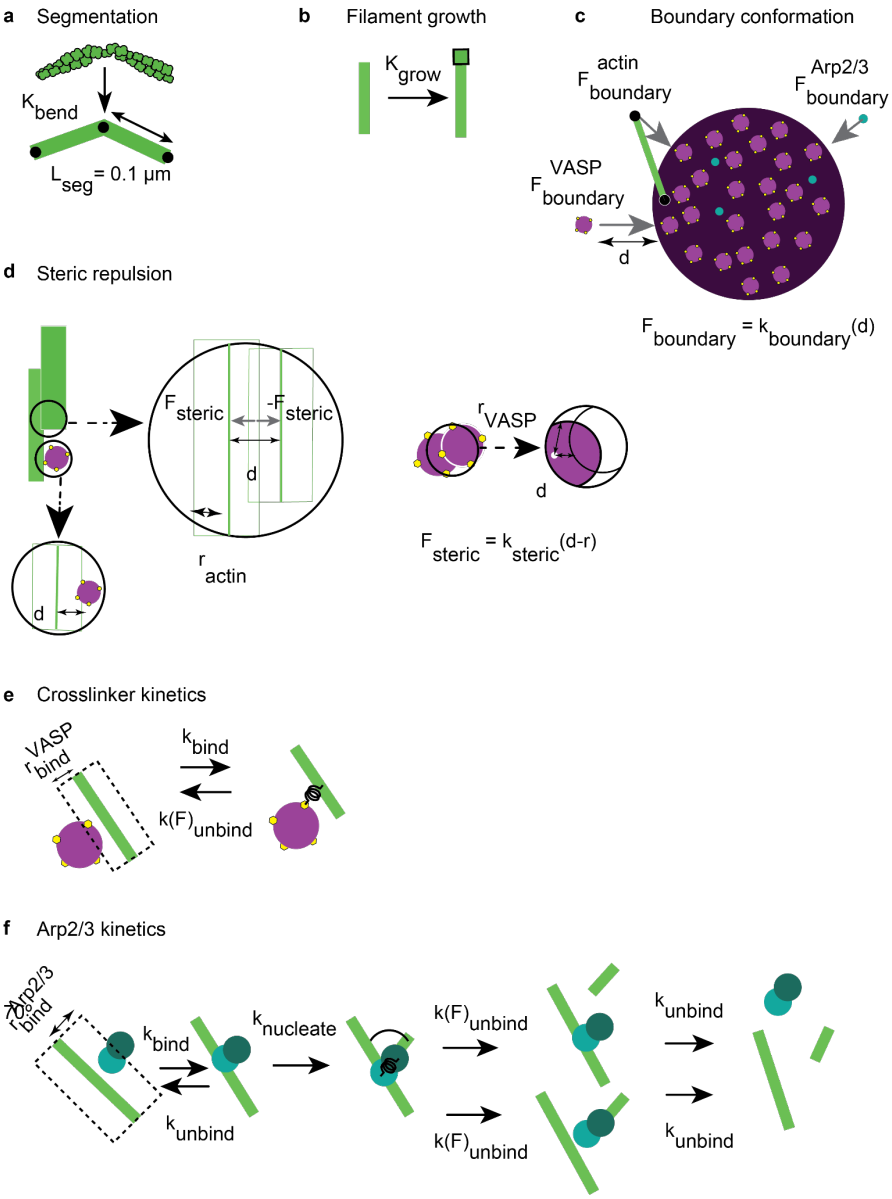

Supplemental Figure S2. Depictions of model parameters. (a) Actin filament curvature is approximated through a series of line segments of length L_{seg}. (b) Propensity of filament growth is calculated from the product of the G-actin monomers available in the volume and the filament growth rate K_{grow}. (c) Actin (green), VASP tetramers (purple spheres), and Arp2/3 (teal) molecules are constrained within the droplet volume through harmonic potentials. (d) Steric repulsion potentials prevent spatial overlap of molecules within the droplet. (e) VASP binding sites (shown as yellow hexagons) located within the binding distance r_{bind}^{VASP} stochastically bind actin filaments at rate k_{bind}. Force sensitive unbinding reaction is also included. (f) Diffusing Arp2/3 molecules within binding distance $r_{bind}^{Arp2/3}$ bind actin stochastically at rate k_{bind}. Branched nucleation at rate $k_{nucleate}$ results in an offspring filament at 70º angle with the parent filament. Force-sensitive unbinding reactions at rate kunbind are also considered. Please refer to Supplementary Table S3 for a detailed table of various parameters used in the model.

Table S3. Table of parameters used to set up the actin model in Cytosim.

Parameter	**Value**		**Notes/Reference**
Total time	600 s		Experimental images are taken at 600s
Implicit evolution time step	0.001 s		
Viscosity of droplet medium	0.5 pN/s m2		100x water
Boundary			
Shape	Sphere	Ellipsoid	
Radius	1 μm	variable	The three axes of the ellipsoid were varied while maintaining the same volume as a sphere.
Boundary repulsion stiffness	200 pN/m for actin filaments and 100pN/m for VASP		This spring stiffness acts on points if they move outside the boundary and the force depends on the distance outside the boundary. Here the stiffness depends on the distance outside the boundary Figure S2C
Actin filaments			
Segmentation length, L_{seg}	100 nm		Figure S2A
Maximum length	2piRdrop m		Rdrop is radius of droplet
Growth rate k_{grow}	0.0103/s		Please refer to Supplementary Methods for details on the filament growth model Figure S2B
Brownian ratchet force for polymerization	10 pN		doi::10.1016/S0006-3495(96)79496-1
Actin flexural rigidity K_{bend}	0.075 pN m2		doi::10.1083/jcb.120.4.923
Actin steric repulsion K_{steric}^{Actin}	Radius 3.5 nm Stiffness 1.0 pN/m		https://doi.org/10.1101/2023.05.26.542517
VASP tetramers	Figure XF		

Radius	30 nm	
Diffusion rate	10 m^2/s	
Concentration of tetramers [VASP-tet]	0.4μM	Varied in this study
Binding rate k_{bind}^{VASP}	1.0 (1/s)	https://doi.org/10.1101/2023.05.26.542517
Binding distance	30 nm	This distance represents the proximity between an actin filament and a VASP molecule required to ensure binding. This value was chosen after a parameter sweep to ensure adequate crosslinking is observed in the simulations.
Valency	4	Each spherical molecule approximates a tetrameric VASP
Unbinding rates k_{unbind}^{VASP}	1.0 (1/s)	https://doi.org/10.1101/2023.05.26.542517
Characteristic unbinding force	10 pN	Typical values for passive crosslinkers
VASP steric repulsion K_{steric}^{VASP}	Radius 30 nm Stiffness 1.0 pN/m	Chosen to ensure ring formation is observed in the kinetic parameters explored in Figure 4
Arp2/3	Figure XG	
Arp2/3 concentration [Arp2/3]	{0, 10, 25, 50, 75, 100, 125, 150} nM	Varied in this study
Binding rate k_{bind}^{Arp}	0.5/s	determined empirically. k_{bind}^{Arp}=0.5/s exhibited 10x increase in the initial number of filaments.
Unbinding rate k_{unbind}^{Arp}	0.005 /s	https://doi.org/10.1073/pnas.191118311
binding distance	12nm~4.72nm+7nm	Arp2/3 radius = 4.72 nm DOI 10.1016/j.str.2008.02.013 Actin diameter = 7 nm https://doi.org/10.1007/BF00713056
Nucleation rate $k_{nucleate}$	0.2/s	https://doi.org/10.1073/pnas.1211164110
branching angle	70^0	10.1073/pnas.95.11.6181

angle stiffness to ensure branching angle	0.076 pN.μm/rad	https://doi.org/10.7554/eLife.49840
Arp2/3-parent filament and Arp2/3-offspring filament unbinding force	6pN	10.1016/S0006-291X(02)00421-7

SUPPLEMENTAL MOVIES

Supplemental Movie M1. VASP droplets formed with Arp2/3 and VCA still undergo fusion.
Supplemental Movie M2. VASP droplets formed with Arp2/3 and VCA still exhibit fast and complete recovery after photobleaching.
Supplemental Movie M3. Simulation time-lapse of droplets with increasing Arp2/3 results in less bundled rings and more central actin accumulation.

SUPPLEMENTAL METHODS

Chemical and mechanical framework employed in CytoSim

Cytosim (https://gitlab.com/f-nedelec/cytosim) is an agent-based framework to simulate cytoskeletal networks with physical realism subject to geometric constraints. In Cytosim, each time step (1ms in this study) involves the evolution of chemical reactions based on their propensities, followed by Brownian dynamics evolution of the chemical species to capture diffusion effects. Filament extension is modeled as follows: Assuming a growth rate of 0.0103/s, we solved the following ordinary differential equations in series to identify the total actin parameter to use in Cytosim [T-Actin].

Symbol	Represents concentration of
[P]	Plus End
[G-actin]	unpolymerized actin
[F-actin]	Polymerized actin
N_{fil}	Number of filaments

$$[T-actin] = [G-actin] + [F-actin] \quad (1)$$

$$\frac{d[F-actin]}{dt} = k_{grow} N_{fil}\left(1 - \frac{[F-actin]}{[T-actin]}\right) \quad (2)$$

These equations were solved with initial conditions $t = 0, N_{fil} = 30, [F-actin](0) = 0.44\,\mu M$ along with boundary conditions $t = 600s, [F-actin](600) = 27.68\,\mu M$. The boundary condition corresponds to per actin filament length of $2\pi\,\mu m$. Solving this numerically in Python using scipy.integrate, we find that [T-actin]=138.38 μM. Please note that while this value is significantly higher than the concentration of actin used in experiments, the value is just one of many degenerate (k_{grow}, [T-actin]) value pairs that would numerically satisfy the equations (1) and (2).

To capture essential chemical reactions observed in VASP droplets, filament extension is modeled as a deterministic force-sensitive process as described above along with stochastic Monte Carlo sampling of crosslinker binding and its force-sensitive unbinding reactions. Arp2/3 binding, nucleation, and unbinding are all modeled as stochastic reactions.

Representation of actin filaments

Actin filaments are represented as inextensible fibers represented as a series of linear segments. The upper limit of segment length is 100 nm. CytoSim computes bending energy of the fiber based on the flexural rigidity specified in the input parameters.

Representation of VASP tetramer

We model VASP as a spherical crosslinker of radius 30 nm with four F-actin binding sites distributed across the surface of the sphere. Cytosim also requires specification of a binding distance parameter between VASP and actin. As we are interested in the changes to ring-shaped actin networks, we used the parameters from our previous study (https://doi.org/10.1101/2023.05.26.542517) that resulted in the formation of ring-shaped networks.

Representation of Arp2/3

Arp2/3 molecules are modeled as diffusing point particles. The binding, nucleation, and unbinding reactions are considered as shown in Supplemental figure S2f. In our simulations, Arp2/3 nucleation produces filaments of 5 nm in length at a 70^o angle with respect to the parent filament.

Position evolution

The diffusion of VASP, points along the actin filaments and Arp2/3 molecules are considered in Cytosim through a Langevin equation framework. For a particle i, the coordinates are given by xi = {xi1, xi2, xi3}. The position along each of the dimensions j is evolved according to the stochastic differential equation given by,

$$dx^{ij}(t) = \mu f^{ij}{}_{tot}(t)\, dt + dB_j(t)$$

Here, μ is the viscosity of solvent, and $f^{ij}{}_{tot}(t)$ represents the total force acting on the particle at time t. The diffusion term (noise) is given by a random variable sampled from a distribution with mean 0 and standard deviation $\sqrt{2D^i dt}$, where the diffusion coefficient is given by $D^i = \mu k_B T$ where T is temperature and k_B is Boltzmann constant. Please refer to Supplementary Table S3 for a detailed description of parameters used in this study.

Analysis of trajectories

Five trajectories were generated for each [Arp2/3] concentration studied. We wanted to understand the distribution of actin within the droplet. Toward this, we discretized the droplet into subvolume shells of varying radii of a finite thickness (δ=25 nm). We calculated the ratio of the local density within shells and the bulk density as,

$$\frac{\rho(r,\delta r)}{\rho(R_{drop})} = \frac{N(r,\delta r)/r^2\delta r}{N_{total}/R^3}$$

Here, N total refers to the total number of actin monomers in the system. $N(r,\delta r)$ represents the number of actin monomers in shell of radius r and thickness δr.

Further, we also calculated the relative actin enrichment (R.A.E) in the core of the droplet using the following equation.

$$R.A.E = \frac{\rho(r_c,\delta r)}{\rho(r_p,\delta r)}$$

where r_c represents the radius a shell in the core of the droplet and r_p represents the radius of a shell in the periphery of the droplet. We chose $r_c = 0.25\ \mu m\ and\ r_p = 0.9\ \mu m$ in this study.